

A class of non-linear adaptive time-frequency transform

Pierre Warion and Bruno Torr sani

Aix-Marseille Univ, CNRS, I2M, Marseille, France.

*Corresponding author(s). E-mail(s): pierre.warion@univ-amu.fr;
Contributing authors: bruno.torresani@univ-amu.fr;

Abstract

This paper introduces a couple of new time-frequency transforms, designed to adapt their scale to specific features of the analyzed function. Such an adaptation is implemented via so-called focus functions, which control the window scale as a function of the time variable, or the frequency variable. In this respect, these transforms are non-linear, which makes the analysis more complex than usual.

Under appropriate assumptions, some norm controls are obtained for both transforms in $L^2(\mathbb{R})$ spaces, which extend the classical continuous frame norm control and guarantees well-definedness on L^2 . Given the non-linearity of the transforms, the existence of inverse transforms is not guaranteed anymore, and is an open question. However, the results of this paper represent a first step towards a more general theory.

Besides mathematical results, some elementary examples of time and frequency focus functions are provided, together with corresponding focused transforms of real and synthetic signals. These can serve as starting point for concrete applications.

Keywords: Time-Frequency analysis, Non-linear transform, time-frequency trade-off, continuous frames

1 Introduction

1.1 Context and purpose

Time-frequency transforms and generalizations (wavelets and others) have long been used in various theoretical and applied domains. Besides quadratic transforms (Wigner

distributions and generalizations), linear transforms such as the Gabor/STFT [1, 2] and wavelet transforms [1, 3–5] generally enjoy simple and useful invertibility properties, and therefore allow describing functions and signals as linear combination of building blocks, called time-frequency atoms. The time (and frequency/scale) resolution of the latter is specified by the construction rule: constant time and frequency resolution for Gabor/STFT, generated by translation and modulation, and constant relative frequency resolution for wavelets, generated by translation and scaling. See also [6–8] for alternative constructions that implement other scaling rules. Variants were also considered in specific applied domains, such as the Stockwell transform [9] in geophysics, which is very close to the constant Q transform [10, 11] we consider below, and the continuous wavelet transform.

In several application domains, in particular audio signal processing, it has been shown that adapting the scale of time-frequency atoms to the content of the signal can provide more efficient signal descriptions [12–14]. The window size is a main control parameter for the time-frequency resolution of the analysis: large windows provide good frequency resolution, while short windows yield good time resolution. The latter is constrained by the uncertainty principle, which can be given various quantitative formulations (see [15, 16] and references therein), and which basically states that precision in time domain is possible at the price of precision loss in frequency domain, and vice versa. The problem of tuning time-frequency resolution as a function of time or frequency has been addressed by various authors, in various contexts, often with pre-defined dependence, sometimes adaptively [13, 14]. As a motivation, even though there is no complete consensus on psycho-physical aspects of human perception, it is known to involve several non-linear effects [17], and it has been claimed that this non-linearity allows going beyond time-frequency uncertainty in terms of localization [18]. Such strategy has been successfully implemented in some advanced audio coders such as AAC (see [19] for a short account), which can switch dynamically between short and long local cosine windows. Another possible motivation can be hyper-resolution (separation of close locally harmonic components or close transients in signals for example). The adaptation is often driven by heuristic computations, for example the optimization of a sparsity criterion of the obtained time-frequency representation, using for example some form of entropy as in [12, 13] or other criteria [14]. The adaptation may be implemented through a time (or frequency) dependent warping function, as in [20]. To our knowledge, the non-linear problem where the time-frequency resolution is adapted to the analyzed function, has not been analyzed from the mathematical point of view so far.

The goal of the present paper is to introduce and study such adaptive time-frequency transforms, able to adapt their time-frequency resolution to the analyzed function. This is done here by introducing a *focus function* $f \mapsto \sigma_f$ which adapts the shape (size, bandwidth etc...) of the analysis window to specific properties of the analyzed signal f . Stepping away from fixed time-frequency resolution makes the analysis significantly more complex. The purpose of this article is to introduce the non-linear transforms, prove that they are well-defined on L^2 and provide explicit, signal-dependent, lower and upper bounds for their norm (which depends on the choice of focus function).

We first introduce in Section 2 a time-focused transform M^τ , which is a modified STFT where the window scale can be adapted to the signal at each time. The adaptation is done by associating with the analyzed signal f a focus function $\sigma_f^\tau : t \mapsto \sigma_f^\tau(t)$. We prove in Theorem 1 the well-definedness of M^τ as a map from $L^2(\mathbb{R})$ into $L^2(\mathbb{R}^2)$ and obtain a norm control of the form $c_f \|f\|^2 \leq \|M^\tau f\|^2 \leq C_f \|f\|^2$, with explicit constants c_f, C_f , under suitable assumptions on the focus function σ_f^τ . Building a frequency-focused STFT can be done along similar lines, and is not addressed here. After briefly reviewing constant-Q transform [11, 21] and continuous wavelet transform [3] and pointing out their relationship, we introduce in Section 3 a new frequency-focused transform M^ν . The latter is built from a complex-valued wavelet transform, modified by a focus function defined in the frequency domain: to the analyzed signal f is associated a focus function $\sigma_f^\nu : \omega \mapsto \sigma_f^\nu(\omega)$. We prove similar norm control and well-definedness results. Explicit examples of focus functions are discussed in the context of continuous time, in Section 2 for time focus, which can be transposed to the frequency focus case. Section 4 is devoted to numerical illustrations, in discrete, finite-dimensional situations. There, we discuss and display examples of focus functions and illustrate the resulting time-focused and frequency-focused spectrograms, computed on real audio signals and toy examples. Section 5 is devoted to conclusions and perspectives.

Except the section devoted to numerical illustrations, the analysis described in the present paper is limited to the continuous time setting and mostly $L^2(\mathbb{R})$. Extensions to more general functional settings and issues related to discretization of the transforms will be the object of further work.

1.2 Notation

We first introduce or recall some notation. We will often use the notation $C([a, b], X)$ for the space of continuous functions from \mathbb{R} into X , supported in $[a, b]$. More generally, given $A \subset \mathbb{R}^{\mathbb{R}}$ we denote by A_c the subspace of functions in A with compact support, and by A_0 the subspace of functions in A which vanish at infinity. We define $A + c := \{f + c, f \in A\}$ for $c \in \mathbb{R}$ and A^+ denotes the subspace of A of non-negative valued functions.

Given an open interval I in \mathbb{R} , $C^n(I)$ stands for the space of function which are n times continuously differentiable on I , and $C^\infty(I) = \bigcap_{n \geq 0} C^n(I)$. Furthermore, we denote by $C_p(I)$ the space of piecewise continuous functions on I , and $C_{p,0}(I)$ the subspace of $C_p(I)$ consisting of functions that tend to 0 at $\pm\infty$. $C_c(I)$ denotes the space of continuous, compactly supported functions on I .

We recall that $L^p(\mathbb{R}^d, d\mu)$, $p \geq 1$, stands for the set of p -integrable functions - where we identify functions that coincide almost everywhere - with respect to the measure μ . The shorter notations $L^p(\mathbb{R}^d)$ and L^p denote respectively $L^p(\mathbb{R}^d, dx)$ and $L^p(\mathbb{R}, dx)$ where dx is the Lebesgue measure.

Given $f \in L^p(\mathbb{R}^d)$, its Fourier transform is either written $\mathcal{F}(f)$ or \hat{f} , and defined by the following convention. For $f \in L^1(\mathbb{R}^d)$,

$$\mathcal{F}(f)(\omega) := \int_{\mathbb{R}^d} f(x) e^{-2i\pi x \cdot \omega} dx, \quad \omega \in \mathbb{R}^d. \quad (1)$$

With this definition, the inverse Fourier transform reads

$$\mathcal{F}^{-1}(F)(t) := \int_{\mathbb{R}^d} F(\omega) e^{2i\pi t \cdot \omega} d\omega, \quad t \in \mathbb{R}^d. \quad (2)$$

For functions of two variables, we introduce the notation

$$\forall x_1, x_2, \xi_1, \xi_2 \in \mathbb{R}, \quad \mathcal{F}_1(f)(\xi_1, x_2) := \int_{\mathbb{R}} f(x_1, x_2) e^{-2i\pi x_1 \xi_1} dx_1; \quad (3)$$

$$\mathcal{F}_2(f)(x_1, \xi_2) := \int_{\mathbb{R}} f(x_1, x_2) e^{-2i\pi x_2 \xi_2} dx_2, \quad (4)$$

and

$$\forall x_1, x_2, \xi_1, \xi_2 \in \mathbb{R}, \quad \mathcal{F}_1^{-1}(F)(x_1, \xi_2) := \int_{\mathbb{R}} F(\xi_1, \xi_2) e^{2i\pi x_1 \xi_1} d\xi_1; \quad (5)$$

$$\mathcal{F}_2^{-1}(F)(\xi_1, x_2) := \int_{\mathbb{R}} F(\xi_1, \xi_2) e^{2i\pi x_2 \xi_2} d\xi_2. \quad (6)$$

2 The non-linear time focused operator

2.1 Atoms and time focused transform

Let us now introduce and study the first non-linear transform of interest here, namely the time focused transform, which involves a focus function defined in the time domain.

Assumptions

Throughout this section we will use the following assumptions.

- i. h is a nonzero, continuous, compactly supported function, called *window*, with length $l \in \mathbb{R}_*^+$. Examples of such a window include most windows used in signal processing (Hann, Blackman,...).
- ii. To every $f \in L^2(\mathbb{R})$ is associated a function σ_f^τ , called *focus function*. σ_f^τ will be assumed to be larger than 1, piecewise continuous and to tend to 1 at infinity, *i.e.*

$$\forall f \in L^2(\mathbb{R}), \quad \sigma_f^\tau \in C_{p,0}^+(\mathbb{R}) + 1. \quad (7)$$

In addition we will assume that for every $f \in L^2$ there is a sequence $(f_n)_n \in (C_c^\infty)^\mathbb{N}$ such that

$$f_n \xrightarrow[n \rightarrow +\infty]{L^2} f \quad \text{and} \quad \sigma_{f_n}^\tau \xrightarrow[n \rightarrow +\infty]{L^\infty} \sigma_f^\tau. \quad (8)$$

In order to lighten the notations we will sometimes omit the subscript τ when there are no ambiguities.

- iii. γ is a C^1 symmetrical diffeomorphism satisfying $\lim_{t \rightarrow -\infty} \gamma(t) = -\infty$ and $\lim_{t \rightarrow +\infty} \gamma(t) = +\infty$.

Remark 1 The technical assumption (8) on the map $f \rightarrow \sigma_f^\tau$ is used in the proof of Lemma 1 below. We believe it should be satisfied for most reasonable choices of mappings $f \rightarrow \sigma_f^\tau$.

Atoms and transform definition

Given the above hypotheses, we can define the time-focused atoms as

$$\forall x, t, \omega \in \mathbb{R}, h_{t, \omega, \sigma_f^\tau}(x) := \sqrt{\gamma'(\omega) \sigma_f^\tau(t)} e^{2i\pi\gamma(\omega)x} h(\sigma_f^\tau(t)(x-t)), \quad (9)$$

and the corresponding transform of a given signal $f \in L^2$ by

$$\forall t, \omega \in \mathbb{R}, M^\tau f(t, \omega) := \langle f, h_{t, \omega, \sigma_f^\tau} \rangle_{L^2}. \quad (10)$$

The pointwise definition of the scalar product is guaranteed by the fact that $h(\sigma_f^\tau(t)(x-t))$ is a continuous, compactly supported function of x . When there are no ambiguities, we will sometimes write $h_{t, \omega, f}$ instead of h_{t, ω, σ_f} and $h_{t, \omega, n}$ instead of $h_{t, \omega, \sigma_{f_n}}$ for a certain sequence $(f_n)_n$.

Remark 2 1. In the definition of time-focused atoms (9), $\sigma_f^\tau(t)$ performs a scaling of the window h around t . We stress that the lower bound 1 of σ_f^τ is purely conventional, and states that rescaled windows cannot be larger than h . The choice of h and the range of values of σ_f^τ therefore determine the overall resolution of the analysis.

2. The function γ performs a mere relabeling of the frequency axis. Examples of γ functions include the obvious choice $\gamma(t) = t$, γ can also be given a kind of hyperbolic sine shape like, which has the effect of compressing high frequencies.

Density result

We first prove the following density result, which states that if we take a L^2 function f and a C_c function f_ε as close as possible to f in L^2 , then the norm of $M^\tau f$ will be controlled by the norm of $M^\tau f_\varepsilon$, which is finite by basic integration rules.

Lemma 1 *Let $f \in L^2(\mathbb{R})$ and $(f_n)_{n \in \mathbb{N}}$ be a sequence such that $f_n \in C_c$ for all $n \in \mathbb{N}$, $f_n \rightarrow f$ in $L^2(\mathbb{R})$ and $\sigma_{f_n}^\tau =: \sigma_n \rightarrow \sigma_f^\tau$ in L^∞ . Then*

$$\forall \varepsilon > 0, \exists N \in \mathbb{N}, \forall n \geq N, \left| \|M^\tau f\|_{L^2} - \|M^\tau f_n\|_{L^2} \right| \leq \varepsilon. \quad (11)$$

Proof Let $\tilde{\varepsilon} > 0$ and $n \in \mathbb{N}$ such that $\|f_n - f\|_{L^2} < \tilde{\varepsilon}$ and $\|\sigma_n - \sigma_f\|_\infty < \tilde{\varepsilon}$. We have

$$\left| \|M^\tau f_n\|_{L^2}^2 - \|M^\tau f\|_{L^2}^2 \right| = \left| \int_{\mathbb{R}^2} |\langle f_n, h_{t, \omega, n} \rangle|^2 d\omega dt - \int_{\mathbb{R}^2} |\langle f, h_{t, \omega, f} \rangle|^2 d\omega dt \right|$$

We first compute, setting $F_n(x, t) := \sqrt{\sigma_n(t)} f_n(x) h(\sigma_n(t)(x-t))$

$$\int_{\mathbb{R}^2} |\langle f_n, h_{t, \omega, n} \rangle|^2 d\omega dt = \int_{\mathbb{R}^4} F_n(x, t) \bar{F}_n(x', t) \gamma'(\omega) e^{2i\pi\gamma(\omega)(x-x')} dx dx' d\omega dt.$$

We recognize the formula of $\mathcal{F}_1^{-1}(F_n)(\gamma(u), t)$, hence

$$\int_{\mathbb{R}^2} |\langle f_n, h_{t, \omega, n} \rangle|^2 d\omega dt = \int_{\mathbb{R}^2} \gamma'(\omega) |\mathcal{F}_1^{-1}(F_n)(\gamma(u), t)|^2 d\omega dt$$

$$\begin{aligned}
&= \int_{\mathbb{R}^2} |\mathcal{F}_1^{-1}(F_n)(u, t)|^2 du dt \\
&= \int_{\mathbb{R}^2} |F_n(x, t)|^2 dx dt = \int_{\mathbb{R}^2} \sigma_n(t) |f_n(x)|^2 h^2(\sigma_n(t)(x-t)) dx dt.
\end{aligned}$$

The same computations give

$$\int_{\mathbb{R}^2} |\langle f, h_{t, \omega, f} \rangle|^2 d\omega dt = \int_{\mathbb{R}^2} \sigma_f(t) |f(x)|^2 h^2(\sigma_f(t)(x-t)) dx dt .$$

We can then write

$$\left| \|M^\tau f_n\|_{L^2}^2 - \|M^\tau f\|_{L^2}^2 \right| = \left| \int_{\mathbb{R}} A(t) dt + \int_{\mathbb{R}} B(t) dt \right| ,$$

with

$$A(t) := \int_{\mathbb{R}} \sigma_f(t) h^2(\sigma_f(t)(x-t)) \left(|f_n(x)|^2 - |f(x)|^2 \right) dx .$$

Therefore,

$$\int_{\mathbb{R}} |A(t)| dt \leq \|\sigma_f\|_\infty \|h\|_\infty \tilde{\varepsilon} .$$

Similarly,

$$B(t) := \int_{\mathbb{R}} \sigma_n(t) |f_n(x)|^2 \left(h^2(\sigma_n(t)(x-t)) - h^2(\sigma_f(t)(x-t)) \right) dx ,$$

thus

$$\int_{\mathbb{R}} |B(t)| dt \leq (\|\sigma_f\|_\infty + \tilde{\varepsilon})(\|f\|_{L^2} + \tilde{\varepsilon})^2 2l \tilde{\varepsilon} .$$

Since $\tilde{\varepsilon}$ is arbitrary, the result follows. \square

When combined with Proposition 2 below, Lemma 1 will show that M^τ is well-defined on L^2 .

Motivations and examples for the time focus function

As stressed in the introduction, it is not the goal of the current paper to discuss in details explicit choices for the focus functions that would be relevant in specific applications. We only provide a couple of prototypical examples, to illustrate desirable and undesirable properties.

Denote by Vf the time-focused transform of $f \in L^2(\mathbb{R})$, with a constant focus function $\sigma(t) = \sigma_{\text{ref}}$ (in other words, a STFT with prescribed time-frequency resolution), and assume for simplicity $\gamma(t) = t$. If the goal is to increase the time resolution of the analysis when the analyzed signal $f \in L^2(\mathbb{R})$ has faster variations, a natural idea could be to consider fixed-time slices of Lf and compute weighted norms of the form

$$\sigma_f^\tau(t) = 1 + \int_{\mathbb{R}} w(\omega) |Vf(\omega, t)| d\omega ,$$

for some weight function w which enhances the contribution of high frequencies (typically $w(\omega) = |\omega|^n$). This quantity is well-defined as soon as $\sup_t \int_{\mathbb{R}} w(\omega) |Vf(\omega, t)| d\omega < \infty$; furthermore, it defines a continuous function that tends to 1 as $t \rightarrow \pm\infty$, since $t \rightarrow Vf(t, \omega)$ may be written as the convolution product of two L^2 functions (up to a phase factor).

However, such a choice is too naive, as the second term is homogenous of degree 1 with respect to f , which results in an increase of the focus function σ when f is multiplied by a constant (in which case one can hardly pretend that the resulting function has factor variations). For these reasons, we will privilege non-linear terms, such as terms involving norm ratios. Natural examples involving such ratio are given by entropies such as the Rényi or Shannon entropies

$$R_\alpha(t) = \frac{1}{1-\alpha} \log \frac{\|Vf(t, \cdot)\|_{L^\alpha}^\alpha}{\|Vf(t, \cdot)\|_{L^1}^\alpha}, \quad H(t) = \lim_{\alpha \rightarrow 1} R_\alpha(t),$$

assuming the above quantities are well defined and nonzero.

Entropy is generally used as a measure of spread (or information content as in [22]): the more spread out the function, the larger the entropy, independently of global normalization. In the context under consideration here, a large value of $R_\alpha(t)$ would indicate that the "energy" of the spectrogram $|Lf(t, \cdot)|$ is spread throughout the whole frequency domain, which can be interpreted in terms of the presence of a transient event in the signal f at time t , and would then require a more time-focused analysis. A corresponding focus function could be defined as

$$\sigma_f^\tau(t) = AR_\alpha(t) + B,$$

for some constants A, B that would control the range of σ_f^τ , or a similar expression using the Shannon entropy. The mathematical analysis of the behavior of such functions defined on the real line is out of the scope of the present paper. We shall discuss adaptations in discrete, finite-dimensional situations, in Section 4 devoted to numerical illustrations.

2.2 Norm relationship

We first express the L^2 norm of Mf in terms of a certain kernel, which guarantees the well-definedness of the transform on L^2 , and will be useful for the rest of the study.

Proposition 1 *Using the previous definition, for $f \in C_c$ we have then*

$$\|M^\tau f\|_{L^2(\mathbb{R}^2)}^2 = \int_{\mathbb{R}^2} \hat{f}(\xi) \bar{\hat{f}}(\xi') K_{\sigma_f^\tau}(\xi - \xi') d\xi d\xi', \quad (12)$$

where the kernel is

$$K_{\sigma_f^\tau}(u) := \int_{\mathbb{R}^2} e^{-2i\pi ut} \bar{\hat{h}}(z) \hat{h}\left(z - \frac{u}{\sigma_f^\tau(t)}\right) dz dt. \quad (13)$$

Proof In order to make notations lighter we use σ for σ_f^τ .

$$\begin{aligned} \|M^\tau f\|_{L^2}^2 &= \int_{\mathbb{R}^2} |\langle \hat{f}, \hat{h}_{t, \omega, \sigma} \rangle|^2 dt d\omega \\ &= \int_{\mathbb{R}^4} \hat{f}(\xi) \bar{\hat{f}}(\xi') \bar{\hat{h}}_{t, \omega, \sigma}(\xi) \hat{h}_{t, \omega, \sigma}(\xi') d\xi d\xi' dt d\omega \end{aligned}$$

$$= \int_{\mathbb{R}^2} \hat{f}(\xi) \bar{\hat{f}}(\xi') \underbrace{\int_{\mathbb{R}^2} \bar{h}_{t,\omega,\sigma}(\xi) \hat{h}_{t,\omega,\sigma}(\xi') dt d\omega d\xi d\xi'}_{=: K_\sigma(\xi, \xi')}$$

We have

$$K_\sigma(\xi, \xi') := \int_{\mathbb{R}^2} \frac{\gamma'(\omega)}{\sigma(t)} e^{-2i\pi(\xi-\xi')t} \bar{h}\left(\frac{\xi-\gamma(\omega)}{\sigma(t)}\right) \hat{h}\left(\frac{\xi'-\gamma(\omega)}{\sigma(t)}\right) d\omega dt .$$

Hence, by setting $y(\omega) = -\frac{\gamma(\omega)}{\sigma(t)}$ we obtain

$$\begin{aligned} K_\sigma(\xi, \xi') &= \int_{\mathbb{R}^2} \bar{h}\left(\frac{\xi}{\sigma(t)} + y\right) \hat{h}\left(\frac{\xi'}{\sigma(t)} + y\right) e^{-2i\pi(\xi-\xi')t} dy dt \\ &= \int_{\mathbb{R}^2} e^{-2i\pi(\xi-\xi')t} \bar{h}(z) \hat{h}\left(z - \frac{\xi-\xi'}{\sigma(t)}\right) dz dt . \end{aligned}$$

The last equality holds by applying the changing of variable $z = y + \frac{\xi}{\sigma(t)}$. And now since the kernel is a function of $\xi - \xi'$ we can deduce the expected result. \square

Corollary 1 *We have, for $f \in C_c(\mathbb{R})$,*

$$\|M^\tau f\|_{L^2(\mathbb{R}^2)}^2 = \int_{\mathbb{R}} |f|^2(t) \mathcal{F}^{-1}(K_{\sigma_f^\tau})(t) dt. \quad (14)$$

Proof The proof uses the Plancherel equality and the fact that the Fourier transform of a convolution product is the product of the Fourier transform. It is an elementary computation

$$\begin{aligned} \|M^\tau f\|_{L^2}^2 &= \int_{\mathbb{R}^2} \hat{f}(\xi) \bar{\hat{f}}(\xi') K_\sigma(\xi - \xi') d\xi d\xi' \\ &= \int_{\mathbb{R}} \hat{f}(\xi) \int_{\mathbb{R}} \bar{\hat{f}}(\xi') K_\sigma(\xi - \xi') d\xi' d\xi \\ &= \langle \hat{f}, K_\sigma * \bar{\hat{f}} \rangle_{L^2_\xi} \\ &= \int_{\mathbb{R}} f(t) \mathcal{F}^{-1}(K_\sigma * \bar{\hat{f}})(t) dt \\ &= \int_{\mathbb{R}} |f|^2(t) \mathcal{F}^{-1}(K_\sigma)(t) dt. \end{aligned}$$

\square

Now we can see that the problem can be solved by controlling the kernel $K_{\sigma_f^\tau}$. In order to obtain such a control, we can introduce the explicit formula of $\mathcal{F}^{-1}(K_{\sigma_f^\tau})$.

$$\forall t \in \mathbb{R}, \mathcal{F}^{-1}(K_{\sigma_f^\tau})(t) = \int_{\mathbb{R}} \sigma_f^\tau(x) |h(\sigma_f^\tau(x)(x-t))|^2 dx. \quad (15)$$

2.3 Main result : norm control

The rest of the section is dedicated to the proof of Theorem 1 below.

Theorem 1 Let $f \in L^2(\mathbb{R})$ and σ_f^τ be a time focus parameter, then

$$c_f \|f\|_{L^2(\mathbb{R})}^2 \leq \|M^\tau f\|_{L^2(\mathbb{R}^2)}^2 \leq C_f \|f\|_{L^2(\mathbb{R})}^2, \quad (16)$$

where

$$c_f = \inf_{t \in \mathbb{R}} \left\{ \int_{\mathbb{R}} |h(x\sigma_f^\tau(x+t))|^2 dx \right\} > 0, \quad (17)$$

and

$$C_f = \int_{\mathbb{R}} |h(\sigma_f^\tau(t))|^2 \sigma_f^\tau(t) dt < \infty. \quad (18)$$

Remark 3 This result is very similar to a continuous frame condition, except that c_f and C_f depend upon the analyzed function f through the focus function σ_f^τ . It is interesting to notice that the non-linearity of the transform only shows up in these constants.

2.4 Upper bound control

In order to prove the upper bound control - which also guarantees the well-definedness in $L^2(\mathbb{R}) \rightarrow L^2(\mathbb{R}^2)$ of our operator - we will control the L^1 norm of the previously introduced kernel $K_{\sigma_f^\tau}$. For now, f denotes a C_c function.

Lemma 2 (L^1 norm control) Let $\sigma(t)$ be a focus function and h be a window function, both as defined in Section 2.1. Let the kernel $K_\sigma(u)$ be defined as in equation (13). Then

$$\int_{\mathbb{R}} K_\sigma(u) du = \int_{\mathbb{R}} |h(\sigma(t)t)|^2 \sigma(t) dt. \quad (19)$$

Proof We have by Fubini's Theorem and setting $u' = z - \frac{u}{\sigma(t)}$,

$$\begin{aligned} \int_{\mathbb{R}} K_\sigma(u) du &= \int_{\mathbb{R}^2} \bar{h}(z) \int_{\mathbb{R}} e^{-2i\pi ut} \hat{h}\left(z - \frac{u}{\sigma(t)}\right) du dz dt \\ &= \int_{\mathbb{R}^2} \bar{h}(z) \int_{\mathbb{R}} e^{-2i\pi\sigma(t)t(z-u)} \hat{h}(u) du \sigma(t) dt dz \\ &= \int_{\mathbb{R}^2} \bar{h}(z) e^{-2i\pi\sigma(t)tz} \int_{\mathbb{R}} \hat{h}(u) e^{2i\pi\sigma(t)tu} du dz \sigma(t) dt \\ &= \int_{\mathbb{R}^2} \bar{h}(z) e^{-2i\pi\sigma(t)tz} h(\sigma(t)t) dz \sigma(t) dt \\ &= \int_{\mathbb{R}} |h(\sigma(t)t)|^2 \sigma(t) dt \end{aligned}$$

□

From Lemma 2 we obtain the upper norm control by introducing a weighed window H_f which lightens a bit the notations.

Proposition 2 (Upper bound) Let $f \in L^2(\mathbb{R})$ and introduce the weighed and rescaled window

$$H_f(t) := |h(\sigma_f^\tau(t)t)| \sqrt{\sigma_f^\tau(t)}, \quad (20)$$

then $H_f \in L^2(\mathbb{R})$ and

$$\|Mf\|_{L^2(\mathbb{R}^2)} \leq \|f\|_{L^2(\mathbb{R})} \|H_f\|_{L^2(\mathbb{R})}. \quad (21)$$

Proof Since h is compactly supported and σ bounded and continuous by part, $H_f \in L^2$. Let us now assume $f \in C_c$. For any $f, g \in L^2$ the dual equality

$$\int_{\mathbb{R}} f(t)\hat{g}(t)dt = \int_{\mathbb{R}} \hat{f}(\omega)g(\omega)d\omega$$

gives

$$\|Mf\|_{L^2}^2 = \int_{\mathbb{R}} \mathcal{F}(|f|^2)(\omega)K_\sigma(\omega)d\omega.$$

As $f \in L^2$ we have $\mathcal{F}(|f|^2) \in L^\infty$, hence by using Lemma 2 for the second member

$$\begin{aligned} \int_{\mathbb{R}} \mathcal{F}(|f|^2)(\omega)K_\sigma(\omega)d\omega &\leq \|\mathcal{F}(|f|^2)\|_{L^\infty} \int_{\mathbb{R}} |h(\sigma(t)t)|^2 \sigma(t)dt, \\ &\leq \|f\|_{L^1}^2 \|H_f\|_{L^2}^2 \\ &= \|f\|_{L^2}^2 \|H_f\|_{L^2}^2. \end{aligned}$$

Using the definition of H_f and taking its L^2 norm we obtain the bound in Proposition 2. Therefore, the upper bound C_f in Theorem 1 equals $\|H_f\|_{L^2}$.

We will now extend the result to L^2 . Let $f \in L^2$, by assumption (8) there exists a sequence $(f_n)_n$ with $f_n \in C_c$, converging to f in L^2 and such that the sequence $(\sigma_{f_n})_n$ converges to σ_f in L^∞ . We know by Lemma 1 that

$$\| \|M^\tau f\|_{L^2} - \|M^\tau f_n\|_{L^2} \| \rightarrow 0 \quad (22)$$

However we know by the upper bound control that

$$\|M^\tau f_n\|_{L^2} \leq \|H_{f_n}\|_{L^2} \|f_n\|_{L^2} \leq \sup_n \{ \|H_{f_n}\|_{L^2} \} \|f_n\|_{L^2} \quad (23)$$

Since σ_{f_n} converges in L^∞ - by assumption (8) - we know that $\sup_n \{ \|H_{f_n}\|_{L^2} \} < \infty$. Hence, $(\|M^\tau f_n\|_n)$ is bounded, and Lemma 1 guarantees that the L^2 norm of $M^\tau f$ for $f \in L^2$ is finite and controlled by $\|f\|_{L^2} C_f = \|f\|_{L^2} \|H_f\|_{L^2}$. \square

The following norm control is not necessary at this point but may be useful in future work, so it is presented here.

Proposition 3 (L^2 norm control) *Let $\sigma(t)$ be a focus function and h be a window function, both as defined in Section 2.1. Let the kernel $K_\sigma(u)$ be defined as in equation (13). Thus we have*

$$\|K_{\sigma_f^\tau}\|_{L^2(\mathbb{R})}^2 = \|h\|_{L^2(\mathbb{R})}^2 \int_{\mathbb{R}} |h(\sigma_f^\tau(t)t)|^2 \sigma_f^\tau(t)^2 dt. \quad (24)$$

Proof Using Fubini's Theorem we obtain

$$\|K_\sigma\|_{L^2}^2 = \int_{\mathbb{R}^4} e^{-2i\pi(u-u')t} |\hat{h}(z)|^2 \hat{h}(z - \frac{u}{\sigma(t)}) \bar{\hat{h}}(z - \frac{u'}{\sigma(t)}) du du' dt dz$$

We set then $x := \frac{u}{\sigma(t)}$ and $x' = \frac{u'}{\sigma(t)}$ which gives

$$\|K_\sigma\|_{L^2}^2 = \int_{\mathbb{R}^2} \underbrace{\left(\int_{\mathbb{R}} e^{-2i\pi x \sigma(t)t} \hat{h}(z-x) dx \right)}_{(1)} \underbrace{\left(\int_{\mathbb{R}} e^{2i\pi x' \sigma(t)t} \hat{h}(z-x') dx' \right)}_{(2)} |\hat{h}(z)|^2 \sigma^2(t) dt dz.$$

We set $x_2 = z - x$ and hence we recognize the inverse Fourier transform formula

$$\begin{aligned} (1) &= \int_{\mathbb{R}} e^{-2i\pi(z-x_2)\sigma(t)t} \hat{h}(x_2) dx_2 \\ &= e^{-2i\pi z \sigma(t)t} h(\sigma(t)t). \end{aligned}$$

Furthermore (2) = $\overline{(1)}$. Thus, when we gather all the members we obtain by Fourier isometry

$$\begin{aligned} \|K_\sigma\|_{L^2}^2 &= \int_{\mathbb{R}^2} |h(\sigma(t)t)|^2 |\hat{h}(z)|^2 dz \sigma(t)^2 dt \\ &= \|h\|_{L^2}^2 \int_{\mathbb{R}} |h(\sigma(t)t)|^2 \sigma(t)^2 dt. \end{aligned}$$

□

2.5 Lower bound control

The following proposition gives a strictly positive lower bound for the norm, in the case of non zero signals.

Proposition 4 (Lower bound) *Let $\sigma(t)$ be a focus function and h be a compactly supported window function, both as defined in Section 2.1. There exists $c = c(\sigma) > 0$ which depends on σ such that*

$$\forall t \in \mathbb{R}, \mathcal{F}^{-1}(K_\sigma)(t) > c, \quad (25)$$

with

$$c := \inf_{t \in \mathbb{R}} \left\{ \int_{\mathbb{R}} |h(x\sigma(x+t))|^2 dx \right\}. \quad (26)$$

Proof Let $t \in \mathbb{R}$. Since $\sigma(x) \geq 1$ for any $x \in \mathbb{R}$, by using equation (15) we have

$$\mathcal{F}^{-1}(K_\sigma)(t) \geq \int_{\mathbb{R}} |h(\sigma(x)(x-t))|^2 dx$$

Hence we have

$$\forall t \in \mathbb{R}, \mathcal{F}^{-1}(K_\sigma)(t) \geq H(t). \quad (27)$$

Now let us prove that $\inf_t H(t) =: c > 0$. We obviously have $H(t) > 0$ for any $t \in \mathbb{R}$ furthermore by the use of the dominated convergence theorem we also have $\lim_{\pm\infty} H(t) > 0$. And since $H(t)$ is continuous (again by the dominated convergence theorem) we can conclude that there exists $c = c(\sigma) > 0$ such that

$$\inf_{t \in \mathbb{R}} H(t) = c > 0. \quad (28)$$

□

Remark 4 Since h is supposed continuous (and nonzero), a lower bound independent of σ can be obtained for c . Without loss of generality, assume that $|h|$ attains its maximum value $\|h\|_\infty$ at the origin. Then there exists $a > 0$ such that for every $y \in (-a, a)$, $|h(y)| > \|h\|_\infty/\sqrt{2}$. Since $\sigma(x) \geq 1$ for all x , we have $x \in (t - a/\sigma(x), t + a/\sigma(x))$ for every $x \in (t - a, t + a)$ so that $(x - t)\sigma(x) \in (-a, a)$. Therefore, we may write

$$\int_{\mathbb{R}} |h(x\sigma(x+t))|^2 dx = \int_{\mathbb{R}} |h((x-t)\sigma(x))|^2 dx \geq \int_{(t-a, t+a)} |h((x-t)\sigma(x))|^2 dx > a\|h\|_\infty^2,$$

which doesn't depend on σ , then on f if $\sigma = \sigma_f^\top$.

Note that the compact support assumption is not necessary for that lower bound.

3 Time frequency transform with frequency focus

It is also interesting to introduce frequency-dependent focus, in addition to time-dependent focus. We first stress that the construction of Section 2 may easily be transposed to that context. Indeed, given the symmetry property of the STFT provided by the Plancherel formula $\langle f, h_{t,\omega} \rangle = \langle \hat{f}, \widehat{h_{t,\omega}} \rangle = \langle \hat{f}, \hat{h}_{\omega,-t} \rangle$, "time-focus" may be applied to the STFT of the Fourier transform \hat{f} of a signal f , resulting in frequency focus. Results similar to the ones described above can be obtained using the very same techniques, we won't address this adaptation here.

We shall rather address the introduction of frequency focus into another transform, which uses scale variables in place of frequency variables, namely wavelet and/or constant-Q transforms. These closely related transforms are based upon time-frequency atoms which have the constant-Q property. The Q factor is usually defined as the ratio of the central frequency ξ of the atom by its spectral bandwidth $\delta\xi$ (both quantities will be properly defined below).

3.1 Continuous constant-Q and wavelet transforms

3.1.1 Transforms on $L^2(\mathbb{R})$

The constant Q transform was introduced in a discrete context [10] and revisited more recently [11, 21]. We provide below a slightly more general version adapted to the continuous setting.

The time-frequency atoms are built from a reference waveform $h \in L^2(\mathbb{R})$, which will be assumed continuous and compactly supported in the Fourier domain. Following the definition from [11, 21], time-frequency atoms $h_{t,u}$ are generated as rescaled and shifted copies of h , which is implemented in the continuous setting as

$$\forall x, t, u \in \mathbb{R}, \quad h_{t,u}(x) := \sqrt{\gamma(u)} e^{2i\pi\gamma(u)x} h(\gamma(u)x - t). \quad (29)$$

Here, γ is a C^1 diffeomorphism such that $\lim_{u \rightarrow -\infty} \gamma(u) = 0$ and $\lim_{u \rightarrow +\infty} \gamma(u) = +\infty$. In [11, 21], γ was given an exponential form, we consider here a slightly more general such scale function. Time-frequency atoms $h_{t,u}$ are normalized so that $\|h_{t,u}\|_{L^2} = \|h\|_{L^2}$ for all t, u . The corresponding constant-Q transform maps every $f \in L^2(\mathbb{R})$ to the function Lf defined by

$$Lf(t, u) = \langle f, h_{t,u} \rangle_{L^2}. \quad (30)$$

Since $f, h \in L^2(\mathbb{R})$, $L_f(t, u)$ is well-defined for all $t, u \in \mathbb{R}$. Under suitable assumptions on h , L also establishes an isometry between $L^2(\mathbb{R})$ and $L^2(\mathbb{R}^2, d\mu)$, where the measure μ is defined by

$$d\mu(t, u) := \frac{\gamma'(u)}{\gamma(u)} du dt . \quad (31)$$

Proposition 5 *Let γ be a C^1 diffeomorphism such that $\lim_{u \rightarrow -\infty} \gamma(u) = 0$ and $\lim_{u \rightarrow +\infty} \gamma(u) = +\infty$, let $h \in L^2(\mathbb{R})$ satisfying the admissibility condition*

$$0 < c_h := \int_{-1}^{+\infty} \frac{|\hat{h}(y)|^2}{y+1} dy = \int_{-\infty}^{-1} \frac{|\hat{h}(y)|^2}{-y-1} dy < \infty . \quad (32)$$

Then for any $f \in L^2(\mathbb{R})$ we have

$$\|L_f\|_{L^2(\mathbb{R}^2, d\mu)}^2 = c_h \|f\|_{L^2(\mathbb{R})}^2 . \quad (33)$$

Sketch of the proof Let $h \in L^2(\mathbb{R})$ satisfying the admissibility condition (32). Assume $f \in C_c(\mathbb{R})$. Then $f \in L^1(\mathbb{R})$, and by Young's convolution inequality $L_f(\cdot, u) \in L^2(\mathbb{R})$ for all $u \in \mathbb{R}$. Introducing the auxiliary function $F(\xi, u) = \hat{f}(\xi) \overline{\hat{h}(\xi/\gamma(u))}$, we have

$$\int_{\mathbb{R}} |L_f(t, u)|^2 dt = \int_{\mathbb{R}^3} F(\xi, u) \overline{F(\xi', u)} e^{2i\pi(\xi - \xi')t/\gamma(u)} d\xi d\xi' dt = \int_{\mathbb{R}} |\check{F}_1(t, u)|^2 dt = \|F(\cdot, u)\|_{L^2}^2 ,$$

where we have used twice Plancherel's formula, and denoted by $\check{F}_1 = \mathcal{F}_1^{-1} F$ the inverse Fourier transform of F with respect to its first variable.

Let $\varepsilon > 0$, $I_\varepsilon = [\gamma^{-1}(1/\varepsilon), \gamma^{-1}(\varepsilon)]$. Focusing on positive frequencies first, consider the (convergent) integral

$$\begin{aligned} \int_{I_\varepsilon} \|F(\cdot, u)\|_{L^2(\mathbb{R}_+)}^2 \frac{\gamma'(u)}{\gamma(u)} du &= \int_{I_\varepsilon \times \mathbb{R}_+} |\hat{f}(\xi)|^2 \left| \hat{\psi} \left(\frac{\xi}{\gamma(u)} - 1 \right) \right|^2 d\xi \frac{\gamma'(u)}{\gamma(u)} du \\ &= \int_{\mathbb{R}_+} |\hat{f}(\xi)|^2 \int_{-1+\xi\varepsilon}^{-1+\xi/\varepsilon} |\hat{h}(y)|^2 \frac{dy}{y+1} . \end{aligned}$$

The inner integral is bounded by the admissibility constant c_h , the dominated convergence theorem then yields

$$\int_{\mathbb{R}} \|F(\cdot, u)\|_{L^2(\mathbb{R}_+)}^2 \frac{\gamma'(u)}{\gamma(u)} du = c_h \|f\|_{L^2(\mathbb{R}_+)}^2 .$$

Similar arguments give, for the negative frequency part,

$$\int_{\mathbb{R}} \|F(\cdot, u)\|_{L^2(\mathbb{R}_-)}^2 \frac{\gamma'(u)}{\gamma(u)} du = c_h \|f\|_{L^2(\mathbb{R}_-)}^2 ,$$

and putting both results together gives Equation (33). Finally, Fatou's lemma gives the extension from $f \in C_c(\mathbb{R})$ to $f \in L^2(\mathbb{R})$. \square

This result bears strong resemblance with known results on continuous wavelet transform [3], in particular the admissibility condition. Notice however that the latter expresses a symmetry condition in the frequency domain with respect to frequency $\xi = -1$, while the corresponding wavelet admissibility condition expresses a similar symmetry with respect to the origin of frequencies. As a consequence, h is necessarily complex-valued.

A closer connection can be made by introducing a function ψ defined by

$$\forall x \in \mathbb{R}, \quad \psi(x) = h(x)e^{2i\pi x} . \quad (34)$$

where ψ can be chosen real valued. Thus, the admissibility condition (32) becomes

$$0 < c_\psi := \int_{\mathbb{R}_+} \frac{|\hat{\psi}(y)|^2}{y} dy = \int_{\mathbb{R}_-} \frac{|\hat{\psi}(y)|^2}{-y} dy < \infty , \quad (35)$$

which is the usual admissibility condition for continuous wavelet transform [23, 24]. We remind that the latter insures invertibility, a left inverse wavelet transform being given by the adjoint operator (up to the constant factor c_ψ^{-1}). The time-frequency atoms can then be written in terms of ψ as

$$\forall x, t, u \in \mathbb{R} , \quad h_{t,u}(x) := \sqrt{\gamma(u)} e^{2i\pi t} \psi(\gamma(u)x - t) , \quad (36)$$

which are closely related to wavelets as defined in [3], with two mild modifications, namely the scale which is labeled by $\gamma(u)$, and a phase factor. These two changes do not modify strongly the classical wavelet transform.

3.1.2 Transforms on $H^2(\mathbb{R})$

The constant-Q and wavelet transforms defined above turn out to be unsuitable for the construction we are about to describe. We found it more convenient to limit to functions whose Fourier transform vanishes for negative frequency. As in [3], we introduce the real Hardy space

$$H^2(\mathbb{R}) = \left\{ f \in L^2(\mathbb{R}), \quad \hat{f}(\xi) = 0 \quad \forall \xi \leq 0 \right\} . \quad (37)$$

Let $\psi \in H^2(\mathbb{R})$. Such a function ψ is called analytic (or progressive) wavelet. The corresponding continuous wavelet transform [3] of a signal $f \in H^2(\mathbb{R})$ is defined by

$$Wf(t, u) = \langle f, \psi_{t,u} \rangle = \frac{1}{\sqrt{\gamma(u)}} \int_{\mathbb{R}_+} \hat{f}(\xi) \bar{\hat{\psi}}\left(\frac{\xi}{\gamma(u)}\right) e^{2i\pi \xi t} d\xi , \quad u, t \in \mathbb{R} . \quad (38)$$

If the admissibility condition below is satisfied

$$0 < c_\psi := \int_{\mathbb{R}_+} \frac{|\hat{\psi}(y)|^2}{y} dy < \infty , \quad (39)$$

the corresponding transform satisfies the following isometry property

$$\|Wf\|_{L^2(\mathbb{R}^2, d\mu)}^2 = c_\psi \|f\|_{H^2}^2 , \quad (40)$$

and the measure is given by

$$d\mu(t, u) = \gamma'(u) du dt . \quad (41)$$

Remark 5 The assumption $f \in H^2(\mathbb{R})$ is not as irrelevant as it may appear. Indeed, in signal processing most signals are real-valued, so that their Fourier transform possess the Hermitean symmetry, *i.e.* $\hat{f}(-\xi) = \overline{\hat{f}(\xi)}$. A real-valued signal $f \in L^2(\mathbb{R})$ is then characterized by its orthogonal projection onto $H^2(\mathbb{R})$, and can be reconstructed as the real part of the latter (up to a factor 2).

3.2 Definition of the frequency-focused transform

We now introduce the frequency focus effect, generated by an associated frequency focus function σ^ν . The role of the focus function is to modify the shape of the analysis waveforms, in a way that depends on some local behavior of the analyzed signal f .

Assumptions

Throughout this section, we make the following assumptions

- i. $\psi \in H^2(\mathbb{R})$ is an analytic wavelet function, therefore satisfying the admissibility condition (39), and such that the quantity below (called frequency localization of ψ) is well-defined.

$$\xi_0 := \frac{1}{\|\psi\|^2} \int_{\mathbb{R}_+} \xi |\hat{\psi}(\xi)|^2 d\xi . \quad (42)$$

In addition, we assume that $|\hat{\psi}|^2$ is differentiable, and make the following technical assumptions:

- $\hat{\psi}(\xi_0) \neq 0$
- There exists $A_\psi > 0$ such that for all $\xi \in \mathbb{R}_+$,

$$\left(|\hat{\psi}|^2 \right)'(\xi) \leq \frac{A_\psi}{|\xi - \xi_0|} . \quad (43)$$

- ii. γ denotes a positive, strictly increasing C^1 diffeomorphism that maps \mathbb{R} onto \mathbb{R}_+^* .
- iii. To every $f \in L^2(\mathbb{R})$ is associated a focus function σ_f^ν of $f \in L^2(\mathbb{R})$, assumed to be continuous, larger than 1 and such that $\sigma_f^\nu - 1$ goes to 0 at $\pm\infty$:

$$\forall f \in L^2(\mathbb{R}), \quad \sigma_f^\nu \in C_0^+(\mathbb{R}) + 1 . \quad (44)$$

Time-frequency atoms and transform

Wavelet and constant-Q transforms use time-frequency atoms with constant relative bandwidth (*i.e.* bandwidth divided by the frequency localization). The frequency-focused transform uses time-frequency atoms with prescribed frequency localization and bandwidth. This requires introducing an appropriate notion of frequency localization. Given a function $f \in H^2(\mathbb{R})$, its frequency localization is defined by extending Equation (42): $\frac{1}{\|f\|_{H^2}^2} \int_{\mathbb{R}_+} \xi |\hat{f}(\xi)|^2 d\xi$ provided the integral is well-defined.

The joint control of bandwidth and frequency localization is achieved by so-called squeezing functions $\xi \rightarrow \beta_u(\xi)$ defined as follows: for every $u \in \mathbb{R}$, we set

$$\beta_u(\xi) = \frac{\sigma_f^\nu(u)}{\gamma(u)} \xi - \xi_1(u) , \quad (45)$$

for some shift parameter $\xi_1(u) > 0$, to be specified below.

Given these parameters, we introduce frequency-focused atoms, defined by their Fourier transform

$$\widehat{\psi_{t,u,\sigma}}(\xi) = \frac{1}{\sqrt{\gamma(u)}} \hat{\psi}(\beta_u(\xi)) e^{-2i\pi\xi t} . \quad (46)$$

A simple calculation shows that $\|\psi_{t,u,\sigma}\|^2 = \|\psi\|^2/\sigma(u)$.

The shift parameters $\xi_1(u)$ are fixed by imposing that the localization of $|\widehat{\psi_{t,u,\sigma}}(\xi)|$ equals $\gamma(u)\xi_0$, which yields

$$\begin{aligned} \gamma(u)\xi_0 &= \frac{1}{\|\psi_{t,u,\sigma}\|^2} \frac{1}{\gamma(u)} \int_{\mathbb{R}_+} \xi \left| \hat{\psi} \left(\frac{\sigma(u)}{\gamma(u)} \xi - \xi_1(u) \right) \right|^2 d\xi \\ &= \frac{1}{\gamma(u)\|\psi_{t,u,\sigma}\|^2} \int_{\mathbb{R}_+} \frac{\gamma(u)}{\sigma(u)} (\zeta + \xi_1(u)) \left| \hat{\psi}(\zeta) \right|^2 \frac{\gamma(u)}{\sigma(u)} d\zeta \\ &= \frac{\gamma(u)}{\|\psi\|^2 \sigma(u)} \left[\int_{\mathbb{R}_+} \zeta \left| \hat{\psi}(\zeta) \right|^2 d\zeta + \xi_1(u) \|\hat{\psi}\|^2 \right] \\ &= \frac{\gamma(u)}{\sigma(u)} [\xi_0 + \xi_1(u)] , \end{aligned}$$

therefore we obtain

$$\xi_1(u) = (\sigma(u) - 1)\xi_0 . \quad (47)$$

Notice that when $u \rightarrow \pm\infty$, $\xi_1(u) \rightarrow 0$ and $\beta_u(\xi) \sim \xi/\gamma(u)$.

The practical effect of such a squeezing is illustrated in Fig. 1, where a squeezing equal to 3 has been applied to three adjacent time-frequency atoms, whose bandwidth is therefore reduced while their amplitude is increased.

Remark 6 1. Since $\xi_0 > 0$ and for all u $\gamma(u) > 0$ and $\sigma(u) \geq 1$, we have that $\beta_u(\xi) < 0$ for all $\xi < 0$; hence $\widehat{\psi_{t,u,\sigma}}(\xi) = 0$ for all $\xi < 0$.

2. The frequency localization may actually be defined in several different ways. For example, assuming that $\hat{\psi}$ is a continuous function, the localization parameter ξ_0 may be defined as the mode of $|\hat{\psi}|$, by setting $\xi_0 = \operatorname{argmax}_{\xi \in \mathbb{R}_+^*} |\hat{\psi}(\xi)|$. In this case, using the same localization measure for $\widehat{\psi_{t,u,\sigma}}$, imposing that $\operatorname{argmax}_{\xi \in \mathbb{R}_+^*} |\widehat{\psi_{t,u,\sigma}}| = \xi_0 \gamma(u)$ is equivalent to $\beta_u(\gamma(u)\xi_0) = \xi_0$, which yields the same expression (47) for the frequency shifts $\xi_1(u)$.

Effect of the squeezing function

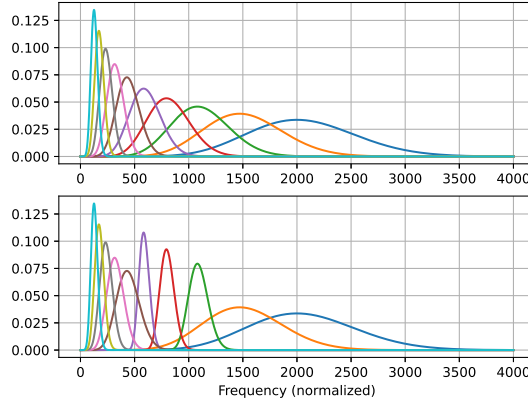


Fig. 1 Frequency squeezing: Fourier transforms of constant-Q atoms (top), and the same atoms out of which three have been squeezed (bottom) by a factor 3.

Given these notations, the frequency-focused transform M^ν can be defined for $f \in C_c$ by

$$\forall t, u \in \mathbb{R}, \quad M^\nu f(t, u) := \langle f, \psi_{t, u, \sigma_f^\nu} \rangle_{L^2}, \quad (48)$$

Plancherel's formula gives the following form

$$M^\nu f(t, u) = \langle \hat{f}, \widehat{\psi_{t, u, \sigma_f^\nu}} \rangle = \frac{1}{\sqrt{\gamma(u)}} \int_{\mathbb{R}_+} \hat{f}(\xi) \overline{\hat{\psi}} \left(\frac{\sigma_f^\nu(u)}{\gamma(u)} \xi - (\sigma(u) - 1) \xi_0 \right) e^{2i\pi \xi t} d\xi \quad (49)$$

Remark 7 Notice that because of our choice of normalization, the time-frequency atoms do not have constant norm any more. Retaining constant norm would impose to normalize them by $\sqrt{\sigma_f}$ instead of σ_f , but this would in turn lead to multiply the measure μ by a factor that depends explicitly on f , which we want to avoid.

Motivations and examples for the frequency focus function

Examples of time focus functions were given in the corresponding paragraph in the previous Section. The rationale for frequency focus functions should follow similar objectives, we won't discuss them here, and refer to Section 4 devoted to numerical experiments.

The main purpose of the next sections is to establish that M^ν can be extended to a well-defined map from $H^2(\mathbb{R}, dx) \rightarrow L^2(\mathbb{R}^2, d\mu)$ satisfying a norm control similar to a frame bound control. The pointwise definition of $M^\nu f(t, u)$ on L^2 is still guaranteed by the fact that $h \in L^2$. Regarding the definition from H^2 into $L^2(\mathbb{R}^2, d\mu)$ we can raise that M^ν is well-defined from C_c into $L^2(\mathbb{R}^2, d\mu)$ and then extend the control by the use of the Fatou's lemma.

Sometimes, if there are no ambiguities, we will write $\psi_{t,u,f}$ instead of ψ_{t,u,σ_f} and $\psi_{t,u,n}$ instead of $\psi_{t,u,\sigma_{f_n}}$ for a certain sequence $(f_n)_n$.

3.3 Kernel and norm relationship

To prove the main result we first derive a norm relationship involving a certain non-negative valued kernel K_σ , so that the study of the norm of $M^\nu f$ will be determined by the norm $\|K_\sigma\|_\infty$.

Proposition 6 *Let ψ satisfying assumptions i. in Section 3.2. Then we have for every $f \in H^2(\mathbb{R})$*

$$\|M^\nu f\|_{L^2(d\mu)}^2 = \int_{\mathbb{R}_+} |\hat{f}(\xi)|^2 K_{\sigma_f^\nu}(\xi) d\xi, \quad (50)$$

where the kernel $K_{\sigma_f^\nu}(\xi)$ is defined by

$$K_{\sigma_f^\nu}(\xi) := \int_{\mathbb{R}_+} \left| \hat{\psi} \left(\beta_{\gamma^{-1}(y)}(\xi) \right) \right|^2 \frac{dy}{y}. \quad (51)$$

Proof We first introduce the auxiliary function $F(\xi, u) = \hat{f}(\xi) \overline{\hat{\psi}(\beta_u(\xi))}$, and notice that $F(\cdot, u) \in L^1(\mathbb{R}_+)$ for all $u \in \mathbb{R}$. Then compute

$$\begin{aligned} \|M^\nu f\|_{L^2(\mathbb{R}^2, d\mu)}^2 &= \int_{\mathbb{R}^2 \times \mathbb{R}_+^2} F(\xi, u) \overline{F(\xi', u)} e^{2i\pi(\xi - \xi')t} \frac{\gamma'(u)}{\gamma(u)} d\xi d\xi' dudt \\ &= \int_{\mathbb{R}^2} \left| (\mathcal{F}_1^{-1} F)(t, u) \right|^2 \frac{\gamma'(u)}{\gamma(u)} dudt \\ &= \int_{\mathbb{R}^2} |F(\xi, u)|^2 \frac{\gamma'(u)}{\gamma(u)} dud\xi \\ &= \int_{\mathbb{R}^2} |\hat{f}(\xi)|^2 \left| \hat{\psi}(\beta_u(\xi)) \right|^2 \frac{\gamma'(u)}{\gamma(u)} dud\xi \\ &= \int_{\mathbb{R}_+^2} |\hat{f}(\xi)|^2 \left| \hat{\psi} \left(\beta_{\gamma^{-1}(y)}(\xi) \right) \right|^2 \frac{dy}{y} d\xi, \end{aligned}$$

where we have denoted by $\mathcal{F}_1^{-1} F$ the inverse Fourier transform of F with respect to its first variable, and then used the corresponding Plancherel formula. The argument above involve the use of Fubini's theorem which is justified by the fact that the integral with respect to y is convergent, this fact is proved in Theorem 2. \square

A simple change of variable gives the following alternative expression for the kernel:

Corollary 2 *The kernel K_σ may be written as*

$$\forall \xi > 0, \quad K_\sigma(\xi) = \int_{\mathbb{R}_+} \left| \hat{\psi} \left(\sigma \circ \gamma^{-1} \left(\frac{\xi}{y} \right) y - \xi_0 \left(\sigma \circ \gamma^{-1} \left(\frac{\xi}{y} \right) - 1 \right) \right) \right|^2 \frac{dy}{y}. \quad (52)$$

Remark 8 If σ is fixed and independent of f , the time-frequency atoms $h_{t,\omega,\sigma(\omega)}$ form a continuous frame of $L^2(\mathbb{R})$ in the terminology of [7, 25]. We will see that in the general case, the assumptions made on σ allow one to stay in a tractable situation.

From now on, the goal is to obtain upper and lower bounds for the kernel K_σ .

3.4 Main result : the L^2 norm control

The main result of this section is the following Theorem 2 which is a generalization to non-linear transform with adaptive window of the classical frame control.

Theorem 2 *Let ψ satisfying assumptions i. in Section 3.2. Let $f \in H^2(\mathbb{R})$, and let $\sigma_f^\nu \in C_0^+(\mathbb{R}) + 1$ denote the associated frequency-focus function. Then we have*

$$d_\psi \|f\|_{L^2(\mathbb{R})}^2 \leq \|M^\nu f\|_{L^2(\mathbb{R}^2, d\mu)}^2 \leq C_{\sigma_f^\nu} \|f\|_{L^2(\mathbb{R})}^2, \quad (53)$$

where $d_\psi > 0$ depends only on the wavelet ψ , and $C_{\sigma_f^\nu}$ is given by

$$C_{\sigma_f^\nu} := c_\psi + A_\psi \int_{\mathbb{R}_+} \left(\sigma_f^\nu(\gamma^{-1}(y)) - 1 \right) \frac{dy}{y} < +\infty, \quad (54)$$

The Theorem is proven in Propositions 7 and 8.

Remark 9 As we shall see in the proof below, the assumptions on ψ insure the existence of an interval (a, b) containing ξ_0 such that $|\hat{\psi}(\xi)|^2 \geq |\hat{\psi}(\xi_0)|^2/2$ for all $\xi \in (a, b)$, which yields the lower bound

$$d_\psi = \frac{|\hat{\psi}(\xi_0)|^2}{2} \ln \left(\frac{b}{a} \right).$$

3.4.1 Upper bound control

We have the following upper bound control.

Proposition 7 *Let $\sigma \in C_0^+(\mathbb{R}) + 1$ be a focus function.*

$$\|K_\sigma\|_\infty \leq c_\psi + A_\psi \int_{\mathbb{R}_+} \left(\sigma(\gamma^{-1}(y)) - 1 \right) \frac{dy}{y}, \quad (55)$$

where A_ψ is given in Equation (43).

Proof Let $\xi \geq 0$ and write $\varphi(\xi) = |\hat{\psi}(\xi)|^2$ for simplicity. We will use the following expression for the kernel, which results from a change of variable,

$$K_\sigma(\xi) = \int_{\mathbb{R}} \varphi(\beta_u(\xi)) \frac{\gamma'(u)}{\gamma(u)} du.$$

Hence, by the mean value theorem, we can write

$$\begin{aligned} K_\sigma(\xi) - c_\psi &= \int_{\mathbb{R}} \left[\varphi(\beta_u(\xi)) - \varphi\left(\frac{\xi}{\gamma(u)}\right) \right] \frac{\gamma'(u)}{\gamma(u)} du \\ &= \int_{\mathbb{R}} \left(\beta_u(\xi) - \frac{\xi}{\gamma(u)} \right) \varphi'(\zeta_{u,\xi}) \frac{\gamma'(u)}{\gamma(u)} du, \end{aligned}$$

with

$$\zeta_{u,\xi} = \xi_0 + \left(\frac{\xi}{\gamma(u)} - \xi_0 \right) (1 + \theta_{u,\xi}(\sigma(u) - 1)), \quad \theta_{u,\xi} \in (0, 1).$$

Since $\beta_u(\xi) - \frac{\xi}{\gamma(u)} = (\sigma(u) - 1) \left(\frac{\xi}{\gamma(u)} - \xi_0 \right)$ and using hypothesis (43) we obtain

$$\begin{aligned} |K_\sigma(\xi) - c_\psi| &\leq \int_{\mathbb{R}} (\sigma(u) - 1) \left| \left(\frac{\xi}{\gamma(u)} - \xi_0 \right) \varphi' \left(\xi_0 + \left(\frac{\xi}{\gamma(u)} - \xi_0 \right) (1 + \theta_{u,\xi}(\sigma(u) - 1)) \right) \right| \frac{\gamma'(u)}{\gamma(u)} du \\ &\leq \int_{\mathbb{R}} (\sigma(u) - 1) \frac{A_\psi}{1 + \theta_{u,\xi}(\sigma(u) - 1)} \frac{\gamma'(u)}{\gamma(u)} du \\ &\leq A_\psi \int_{\mathbb{R}} (\sigma(u) - 1) \frac{\gamma'(u)}{\gamma(u)} du \\ &= A_\psi \int_{\mathbb{R}^+} \left(\sigma(\gamma^{-1}(y)) - 1 \right) \frac{dy}{y}, \end{aligned}$$

which achieves the proof of the Proposition. \square

3.4.2 Lower bound control

The following result guarantees the existence of a positive lower bound that only depends on the wavelet ψ . Under the hypothesis i. in Section 3.2, we have the existence of $a < b \in \mathbb{R}_+^*$ such that

$$\forall y \in (a, b), |\hat{\psi}(y)|^2 \geq \frac{|\hat{\psi}(\xi_0)|^2}{2}. \quad (56)$$

We can then prove

Proposition 8 *Let $\sigma \in C_0^+(\mathbb{R}) + 1$ be a focus function. Then*

$$\forall \xi > 0, K_\sigma(\xi) \geq \frac{|\hat{\psi}(\xi_0)|^2}{2} \ln \left(\frac{b}{a} \right). \quad (57)$$

Proof Let us fix $\xi > 0$. Using the notation

$$\alpha_\xi(y) = \beta_{\gamma^{-1}(y)}(\xi) = \left(\sigma \circ \gamma^{-1} \right) (y) \frac{\xi}{y} - \xi_0 \left(\left(\sigma \circ \gamma^{-1} \right) (y) - 1 \right),$$

we can write

$$K_\sigma(\xi) = \int_{\mathbb{R}_+} |\hat{\psi}(\alpha_\xi(y))|^2 \frac{dy}{y}.$$

Since α_ξ is continuous, we have

$$\begin{aligned} \alpha_\xi((\xi/b, \xi/a)) &\supset (\alpha_\xi(\xi/b), \alpha_\xi(\xi/a)) \\ &= \left((a - \xi_0) \left(\sigma \circ \gamma^{-1} \right) (1/a) + \xi_0, (b - \xi_0) \left(\sigma \circ \gamma^{-1} \right) (1/b) + \xi_0 \right) \\ &\supset (a, b). \end{aligned}$$

Indeed, since $a - \xi_0 < 0$ and $b - \xi_0 > 0$, together with the fact that $\sigma(u) \geq 1$ for all u , we have

$$\begin{aligned} (a - \xi_0) \left(\sigma \circ \gamma^{-1} \right) (1/a) &\leq a - \xi_0, \\ (b - \xi_0) \left(\sigma \circ \gamma^{-1} \right) (1/b) &\geq b - \xi_0. \end{aligned}$$

Hence

$$\begin{aligned}
\int_{\mathbb{R}^+} |\hat{\psi}(\alpha_\xi(y))|^2 \frac{dy}{y} &\geq \frac{|\hat{\psi}(\xi_0)|^2}{2} \int_{\alpha_\xi^{-1}((a,b))} \frac{dy}{y} \\
&\geq \frac{|\hat{\psi}(\xi_0)|^2}{2} \int_{\xi/b}^{\xi/a} \frac{dy}{y} \\
&\geq \frac{|\hat{\psi}(\xi_0)|^2}{2} \ln\left(\frac{b}{a}\right),
\end{aligned}$$

which proves the proposition, and yields the expression of the bound given in Remark 9. \square

4 Numerical illustrations

We provide in this section illustrations of the frequency and time focus functions introduced in the core of the paper. We stress that these do not intend to address specific applied problems, but simply to show that such focus functions can indeed be designed and achieve well targeted goals.

Stepping from continuous time functions to discrete signals requires choosing a discretization scheme. Our approach here was to limit ourselves to uniform, frequency or scale independent, time sampling. In other words, we stick to very redundant time-frequency/scale transforms, and do not address discretization issues such as the ones developed in classical frame theory, which we consider beyond the scope of this paper.

4.1 Illustration of time focus

We illustrate the time focus effect using a simple example of time focus function, applied to a real audio signal. For the sake of simplicity, we take $\gamma(\omega) = \omega$ for all $\omega \in \mathbb{R}$. Given some signal $f \in L^2(\mathbb{R})$, we denote by $Vf = M_{\sigma_{\text{ref}}}^\tau f$ the transform of f , with a focus function uniformly equal to a reference scale σ_{ref} , and define

$$\sigma_f^\tau(t) = A \int \omega^n |Vf(t, \omega)| d\omega + B, \quad (58)$$

where $n \in \mathbb{N}$ is a fixed integer, and $A, B > 0$ are real constants that can be adjusted so that for all t ,

$$1 \leq \sigma_f^\tau(t) \leq \sigma_{\text{max}},$$

for some prescribed maximal focus σ_{max} .

We display in Fig. 2 a 3.5 seconds excerpt from a castanet sound recording (from the SQAM assessment database [26]), and the corresponding focus function estimated using Equation (58). The window h was a 10 milliseconds long truncated Gaussian window (to enforce compact support), and parameters were set to $n = 1$, $\sigma_{\text{ref}} = 1$ and $\sigma_{\text{max}} = 5$. As can be seen, the transients are well detected. Fig. 3 represents the spectrograms obtained with the unfocused transform ($\sigma(t) = 1$ for all t), and the focused transform. The latter features sharper attacks, the intervals in between attacks being unchanged.

This example is quite an easy one, as the signal only contains transients. The same focus function performs worse on a slightly more complex signal, that features

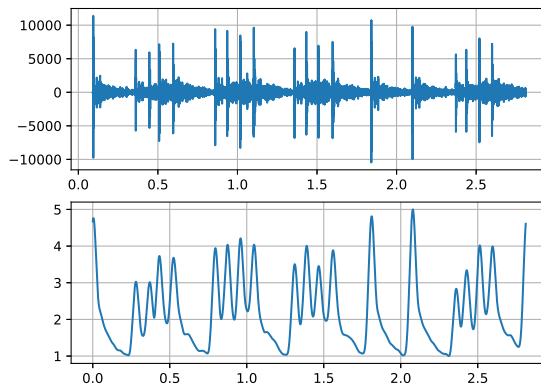


Fig. 2 Castanet signal and corresponding time focus function, defined by Equation (58)

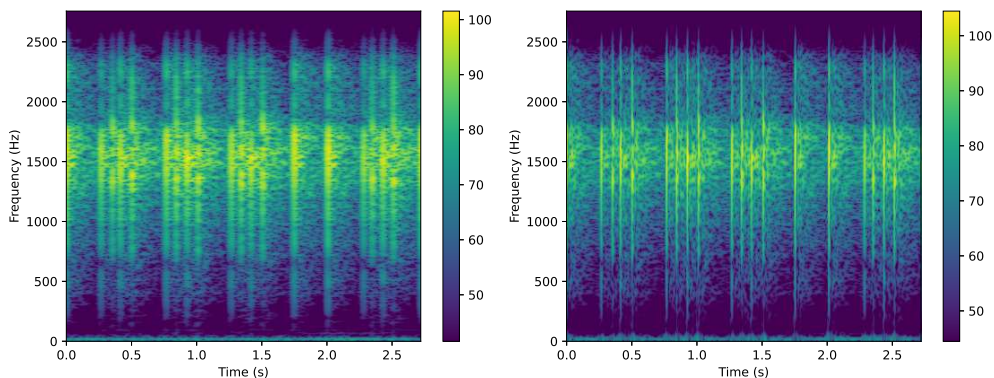


Fig. 3 Log-spectrograms for the castanet signal plotted in Fig. 2. Left: unfocused; Right: focused, using the focus function defined in (58) with parameters given in the text.

significant harmonic components together with transients. We display in Fig. 4 a 3.5 seconds excerpt from a glockenspiel sound recording (available from the companion web site of [12]), together with the corresponding focus function (bottom left-hand panel). As can be seen, the time focus function (58) detects the attacks of notes, but the decay is much slower than it was for the castanet signal, and the focus effect on the resulting spectrogram (not shown here) is not satisfactory. In fact, the focus function in (58) is indeed sensitive to transients, but also on the local energy of the signal. Increasing the value of n does not seem to improve.

As an alternative, we display in the bottom right-hand panel of Fig. 4 the focus function based upon the entropy of fixed-time slices of the reference spectrogram

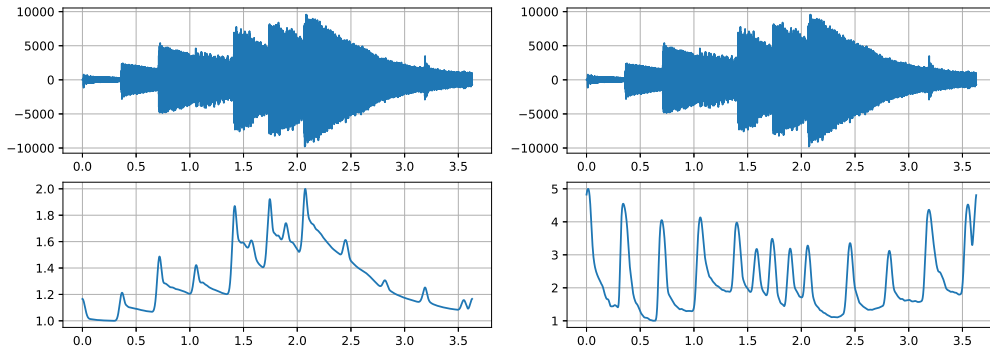


Fig. 4 Glockenspiel signal (top) and corresponding time focus functions. Left: focus function as defined in Equation (58). Right: focus function as defined in Equation (59).

(suitably normalized to unit norm).

$$\sigma_f(t) = -A \int |\tilde{V}f(t, \omega)| \log |\tilde{V}f(t, \omega)| d\omega + B, \quad (59)$$

where $\tilde{V}f(t, \omega) = Vf(t, \omega) / \|Vf(t, \cdot)\|_{L^1(\mathbb{R}, d\omega)}$. Parameters A and B were again set to ensure $1 \leq \sigma(t) \leq \sigma_{\max} = 5$.

The rationale is that slices that do not correspond to transient events exhibit a sparser behavior, and can therefore be expected to possess a small entropy. The right-hand panel of Fig. 4 shows that the estimated focus function is indeed sensitive to transients, independently of the local amplitude (which is clear from the construction in (59)). The corresponding spectrograms are displayed in Fig. 5, from which a better focus effect can be seen on the transient attacks of the instrument. However, the sustained parts have lost their frequency resolution in parts of the signal featuring close transients (in the middle segment of the signal).

Entropy seems to be a valuable choice for building a time focus function. Let us nevertheless stress that the construction depends on several parameters, including the reference focus σ_{ref} involved in the reference STFT Vf , and the maximal allowed value σ_{\max} . One may also investigate extensions built upon Renyi entropies, which provide different measures of spreading in the time-frequency domain, as shown in [12].

4.2 Illustration of frequency focus

We now illustrate the behavior of the frequency-focused transform. Again, we will build a focus function using an entropy measure, based upon fixed-frequency slices of a standard continuous wavelet transform

$$\sigma(u) = -A \int |\tilde{W}f(t, u)| \log |\tilde{W}f(t, u)| du + B, \quad (60)$$

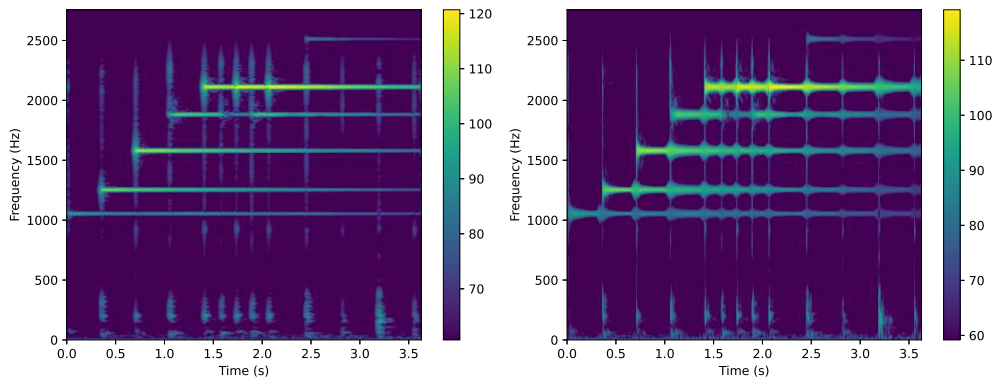


Fig. 5 Spectrograms for the glockenspiel signal and focus function plotted in the right hand panel of Fig. 4. Left: unfocused; Right: focused, using the entropy-based focus function defined in (59).

where $\widetilde{W}f(t, u) = Wf(t, u) / \|Wf(\cdot, u)\|_{L^1(\mathbb{R})}$ is a normalized continuous wavelet transform (equivalently a frequency-focused transform with focus function uniformly equal to $\sigma_{\text{ref}} = 1$). We have chosen here the simplest choice $\gamma(u) = e^u$. Again, A and B are parameters which are adjusted so that $1 \leq \sigma(u) \leq \sigma_{\text{max}}$, for all u and for some prescribed maximal focus σ_{max} . We display in Fig. 6 the simulated signal and its peri-

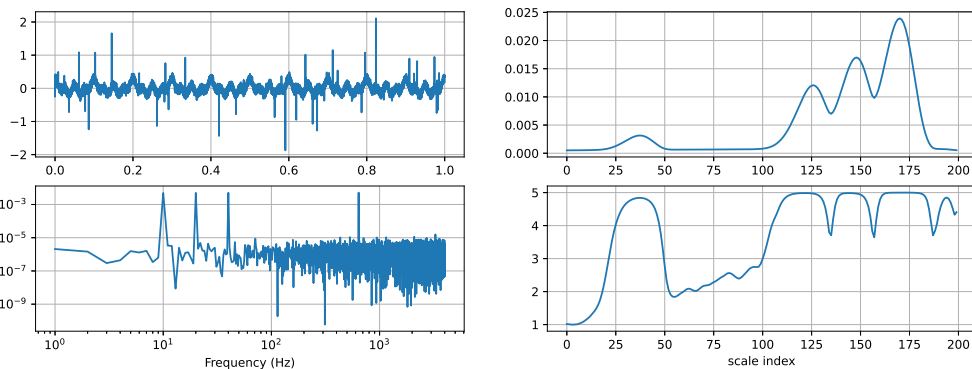


Fig. 6 Left: toy signal (top) and periodogram (bottom, loglog scale). Right: wavelet spectrum of the simulated signal and corresponding frequency focus function as defined in Equation (60).

odogram (square modulus of Fourier transform) on the left, and its wavelet spectrum and the frequency focus. The simulated signal is composed of the sum of four sine waves at different frequencies with equal amplitudes, randomly located spikes with random amplitudes (50 spikes) and Gaussian white noise. The wavelet spectrum is defined as the time-average of the continuous wavelet transform modulus displayed in Fig. 7, left panel.

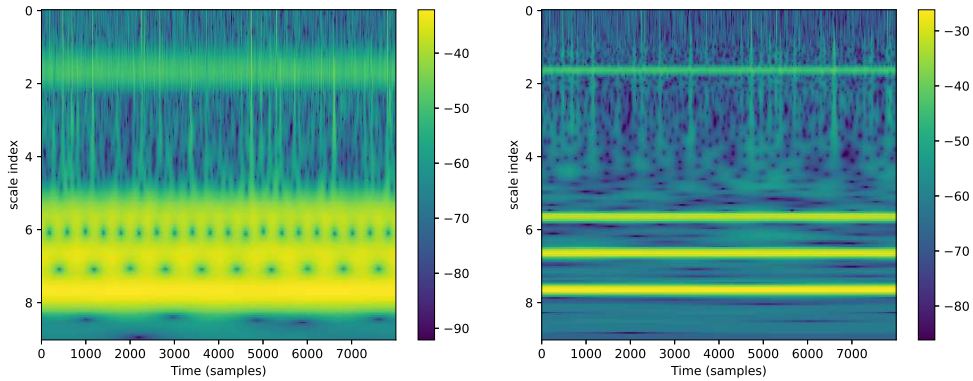


Fig. 7 Scalograms for the glockenspiel signal and frequency focus function plotted in Fig. 6. Left: unfocused; Right: focused, using the entropy-based focus function defined in (60).

Obviously, the frequency focus is insensitive to the different amplitudes of the four sine waves in the wavelet domain. The resulting effect is visible on the scalograms (modulus of time-scale transforms) on the right panel of Fig. 7, where the frequency resolution has clearly been increased for displaying the four sine waves, and is weakly changed elsewhere, in particular at smallest scales. It is also worth observing that the localization of spikes at small scales from wavelet maxima appears simpler, since these lines of maxima are less affected by the presence of the sine wave. We didn't consider a real example for illustrating the frequency focus, since constant amplitude sine waves rarely appear in real signals. Most often, sine waves start at a given time and their amplitude decays with time, which is not accounted for by the simple criterion illustrated here. The latter could be adapted to be used inside time segments, after a prior time segmentation. Such an extension would however require additional modeling work, and is beyond the scope of this paper.

5 Conclusion

We introduced in this paper new time-scale-frequency transforms that can adapt their time-frequency resolution to the analyzed signal, through the frequency domain and time domain focus functions $f \rightarrow \sigma_f^y$ and $f \rightarrow \sigma_f^x$. Based upon short time Fourier transform or continuous wavelet transform, the proposed transforms adapt dynamically the scale/bandwidth of analysis windows or wavelet as a function of frequency or time, leading to non-linear transforms. Under suitable assumptions on focus functions, we could prove first important results on the transforms such as the well-definedness on L^2 , and norm controls similar to the one obtained in the linear case.

In Theorems 1 and 2, we obtain a control of the type

$$\sup_{\substack{f \in L^2(\mathbb{R}) \\ f \neq 0}} \frac{\|Mf\|_{L^2}}{\|f\|_{L^2}} = \sup_{\substack{f \in L^2(\mathbb{R}) \\ f \neq 0}} C_f^{1/2},$$

where C_f depends on $f \in L^2(\mathbb{R})$ only through the focus function σ_f . More specific assumptions on the focus functions are needed to insure a finite upper bound for C_f with $f \in L^2$. For example, one may specify that $1 \leq \sigma_f \leq \sigma_{\max}$ for some prescribed σ_{\max} , as we did in numerical illustrations. It would be interesting to study more thoroughly generic mappings $f \rightarrow \sigma_f$ and derive sufficient conditions insuring the finiteness of C_f .

Note that, due to the non-linearity of the transform, the above quantity doesn't define a norm for the transform. Lipschitz continuity, *i.e.* the existence of a constant $C(M)$ such that

$$\forall f_1, f_2 \in L^2, \quad \|Mf_1 - Mf_2\|_{L^2} \leq C(M)\|f_1 - f_2\|_{L^2} \quad (61)$$

would clearly be of interest too (see also generalized operator norms introduced and studied in [27]). Proving the existence of such Lipschitz constants for M^ν and M^τ would ensure their uniform continuity. However, none of the two above mentioned results is strong enough to prove the existence of a Lipschitz constant that satisfies Equation (61). We plan to follow this line in the near future.

Of interest too for the inversion of the non-linear transforms would be to investigate which conditions would guarantee the existence of a constant $c(M)$ such that

$$\forall f_1, f_2 \in L^2(\mathbb{R}), \quad c(M)\|f_1 - f_2\|_{L^2} \leq \|Mf_1 - Mf_2\|_{L^2}. \quad (62)$$

Such property would guarantee injectivity of the non-linear transform. Again, the lower bounds provided in Theorems 1 and 2 are not sufficient to yield directly injectivity, even though the bound does not depend on the analyzed function f .

A main further goal will be to study the invertibility of such non-linear transforms. From our results, inverse transforms can be obtained if both the transform Mf and the focus function σ_f are known, but not in situations where only the transform Mf is known. A first step would be to analyze in which conditions an approximate inverse can be obtained when an approximation of the focus function is available. The above-mentioned problems are likely to play a role for this question. This may open the door to iterative inversion methods.

Last but not least, we plan to head to concrete applications of this approach, in particular in the context of audio perception modelling, which was one of the main motivations for this work. For that, we plan to investigate further focus functions that could be relevant in applications, starting from the simple models and examples described in Section 4, and study more thorough applications to real signals.

Additional information

On behalf of all authors, the corresponding author states that there is no conflict of interest. This work didn't benefit from any specific funding. No data is associated to this work. Authors contributed equally to this work.

References

- [1] Daubechies, I.: Ten Lectures on Wavelets. CBMS-NSF Regional Conference Series in Applied Mathematics, vol. 61. Society for Industrial and Applied Mathematics, USA (1992). <https://doi.org/10.1137/1.9781611970104.fm>
- [2] Gröchenig, K.: Foundations of Time-frequency Analysis. Springer, Boston, MA (2013). <https://doi.org/10.1007/978-1-4612-0003-1>
- [3] Grossmann, A., Morlet, J.: Decomposition of Hardy functions into square integrable wavelets of constant shape. SIAM Journal on Mathematical Analysis **15**(4), 723–736 (1984) <https://doi.org/10.1137/0515056>
- [4] Mallat, S.: A Wavelet Tour of Signal Processing, Third Edition: The Sparse Way. Academic Press, Inc., USA (2008). <https://doi.org/10.1016/B978-0-12-374370-1.X0001-8>
- [5] Meyer, Y.: Wavelets and Operators. Cambridge Studies in Advanced Mathematics, vol. 1. Cambridge University Press, Cambridge, UK (1993). <https://doi.org/10.1017/CBO9780511623820>
- [6] Kalisa, C., Torrèsani, B.: N-dimensional affine Weyl-Heisenberg wavelets. Annales de l’I.H.P. Physique théorique **59**(2), 201–236 (1993) <https://eudml.org/doc/76620>
- [7] Ali, S.T., Antoine, J.-P., Gazeau, J.-P.: Coherent States, Wavelets and Their Generalizations. Springer, New York, Berlin, Heidelberg (2000). <https://doi.org/10.1007/978-1-4614-8535-3>
- [8] Fornasier, M.: Banach frames for α -modulation spaces. Applied and Computational Harmonic Analysis **22**(2), 157–175 (2007) <https://doi.org/10.1016/j.acha.2006.05.008>
- [9] Stockwell, R.G., Mansinha, L., Lowe, R.P.: Localization of the complex spectrum: the S transform. IEEE Transactions on Signal Processing **44**(4), 998–1001 (1996) <https://doi.org/10.1109/78.492555>
- [10] Brown, J.C.: Calculation of a constant Q spectral transform. The Journal of the Acoustical Society of America **89**(1), 425–434 (1991) <https://doi.org/10.1121/1.400476>
- [11] Velasco, G.A., Holighaus, N., Dörfler, M., Grill, T.: Constructing an invertible constant-Q transform with non-stationary Gabor frames. Proceedings of DAFX11, Paris **33** (2011)
- [12] Jaillet, F., Torrèsani, B.: Time-frequency jigsaw puzzle: adaptive multiwindow

- and multilayered Gabor expansions. *International Journal of Wavelets, Multiresolution and Information Processing* **05**(02), 293–315 (2007) <https://doi.org/10.1142/S0219691307001768> <https://doi.org/10.1142/S0219691307001768>
- [13] Liuni, M., Robel, A., Matusiak, E., Romito, M., Rodet, X.: Automatic adaptation of the time-frequency resolution for sound analysis and re-synthesis. *IEEE Transactions on Audio, Speech, and Language Processing* **21**(5), 959–970 (2013) <https://doi.org/10.1109/TASL.2013.2239989>
- [14] Leiber, M., Marnissi, Y., Barrau, A., Badaoui, M.E.: Differentiable adaptive short-time Fourier transform with respect to the window length. In: *ICASSP 2023 - 2023 IEEE International Conference on Acoustics, Speech and Signal Processing (ICASSP)*, pp. 1–5 (2023). <https://doi.org/10.1109/ICASSP49357.2023.10095245>
- [15] Folland, G.B., Sitaram, A.: The uncertainty principle: A mathematical survey. *Journal of Fourier Analysis and Applications* **3**, 207–238 (1997) <https://doi.org/10.1007/BF02649110>
- [16] Ricaud, B., Torrèsani, B.: Refined support and entropic uncertainty inequalities. *IEEE Transactions on Information Theory* **59**(7), 4272–4279 (2013) <https://doi.org/10.1109/TIT.2013.2249655>
- [17] Oxenham, A.J.: How we hear: The perception and neural coding of sound. *Annual Review of Psychology* **69**(1), 27–50 (2018) <https://doi.org/10.1146/annurev-psych-122216-011635> . PMID: 29035691
- [18] Oppenheim, J.N., Magnasco, M.O.: Human time-frequency acuity beats the Fourier uncertainty principle. *Phys. Rev. Lett.* **110**, 044301 (2013) <https://doi.org/10.1103/PhysRevLett.110.044301>
- [19] Brandenburg, K.: MP3 and AAC Explained. In: *Audio Engineering Society Conference: 17th International Conference: High-Quality Audio Coding* (1999). <http://www.aes.org/e-lib/browse.cfm?elib=8079>
- [20] Holighaus, N., Wiesmeyr, C., Balazs, P.: Continuous warped time-frequency representations—coorbit spaces and discretization. *Applied and Computational Harmonic Analysis* **47**(3), 975–1013 (2019) <https://doi.org/10.1016/j.acha.2018.03.002>
- [21] Holighaus, N., Dörfler, M., Velasco, G.A., Grill, T.: A framework for invertible, real-time constant-Q transforms. *IEEE Transactions on Audio, Speech, and Language Processing* **21**(4), 775–785 (2012) <https://doi.org/10.1109/TASL.2012.2234114>
- [22] Baraniuk, R.G., Flandrin, P., Janssen, A.J.E.M., Michel, O.J.J.: Measuring time-frequency information content using the renyi entropies. *IEEE Transactions on*

- Information Theory **47**(4), 1391–1409 (2001) <https://doi.org/10.1109/18.923723>
- [23] Grossmann, A., Morlet, J., Paul, T.: Transforms associated to square integrable group representations. I: general results. *Journal of Mathematical Physics* **26**(10), 2473–2479 (1985) <https://doi.org/10.1063/1.526761>
- [24] Grossmann, A., Morlet, J., Paul, T.: Transforms associated to square integrable group representations. II: examples. *Annales de l’I.H.P. Physique théorique* **45**(3), 293–309 (1986)
- [25] Dahlke, S., Fornasier, M., Rauhut, H., Steidl, G., Teschke, G.: Generalized coorbit theory, banach frames, and the relation to α -modulation spaces. *Proceedings of the London Mathematical Society* **96**(2), 464–506 (2008) <https://doi.org/10.1112/plms/pdm051>
- [26] European Broadcasting Union: Sound quality assessment material: Recordings for subjective tests. (1988). Tech 3253. <https://tech.ebu.ch/publications/tech3253>
- [27] Wei, W.H.: On the development of nonlinear operator theory. *Functional Analysis and Its Applications* **54**, 49–52 (2020) <https://doi.org/10.1134/S0016266320010062>

